Sequential Prostate Magnetic Resonance Imaging in Newly Diagnosed High-risk Prostate Cancer Treated with Neoadjuvant Enzalutamide is Predictive of Therapeutic Response

Fatima Karzai[1], Stephanie M. Walker[2], Scott Wilkinson[3], Ravi A. Madan[1], Joanna H. Shih[4], Maria J. Merino[5], Stephanie A. Harmon[6], David J. VanderWeele[3], Lisa M. Cordes[1], Nicole V. Carrabba[3], John R. Bright[3], Nicolas T. Terrigino[3], Guinevere Chun[1], Marijo Bilusic[1], Anna Couvillon[1], Amy Hankin[1], Monique N. Williams[1], Rosina T. Lis[7], Huihui Ye[8], Peter L. Choyke[2], James L. Gulley[1], Adam G. Sowalsky[3], Baris Turkbey[2], Peter A. Pinto[9], and William L. Dahut[1]

ABSTRACT

Purpose: For high-risk prostate cancer, standard treatment options include radical prostatectomy (RP) or radiotherapy plus androgen deprivation therapy (ADT). Despite definitive therapy, many patients will have disease recurrence. Imaging has the potential to better define characteristics of response and resistance. In this study, we evaluated prostate multiparametric MRI (mpMRI) before and after neoadjuvant enzalutamide plus ADT.

Patients and Methods: Men with localized intermediate- or high-risk prostate cancer underwent a baseline mpMRI and mpMRI-targeted biopsy followed by a second mpMRI after 6 months of enzalutamide and ADT prior to RP. Specimens were sectioned in the same plane as mpMRI using patient-specific 3D-printed molds to permit mpMRI-targeted biopsies to be compared with the same lesion from the RP. Specimens were analyzed for imaging and histologic correlates of response.

Results: Of 39 patients enrolled, 36 completed imaging and RP. Most patients (92%) had high-risk disease. Fifty-eight lesions were detected on baseline mpMRI, of which 40 (69%) remained measurable at 6-month follow-up imaging. Fifty-five of 59 lesions (93%) demonstrated >50% volume reduction on posttreatment mpMRI. Three of 59 lesions (5%) demonstrated growth in size at follow-up imaging, with two lesions increasing more than 3-fold in volume. On whole-mount pathology, 15 patients demonstrated minimal residual disease (MRD) of <0.05 cc or pathologic complete response. Low initial mpMRI relative tumor burden was most predictive of MRD on final pathology.

Conclusions: Low relative lesion volume at baseline mpMRI was predictive of pathologic response. A subset of patients had limited response. Selection of patients based on these metrics may improve outcomes in high-risk disease.

Introduction

Prostate cancer is the second leading cause of cancer-related death in individuals who are born biologically male in the United States, with an estimated 191,930 new cases and 33,330 deaths in 2020 (1). While radical prostatectomy or radiotherapy are potentially curative modalities for patients with localized disease, 20%–40% of patients treated with radical prostatectomy or radiotherapy will ultimately develop castration-resistant prostate cancer (2). It is imperative to evaluate new treatment strategies, particularly in individuals with high-risk disease. Androgen deprivation therapy (ADT), combined with newer generation androgen receptor (AR) axis inhibitors, such as abiraterone and enzalutamide, is widely used in metastatic castration-resistant prostate cancer (3, 4), metastatic castration-sensitive prostate cancer (5), and nonmetastatic castration-resistant prostate cancer (6). More recent studies have shown promise in reducing tumor burden and cancer stage in the neoadjuvant setting, prior to radical prostatectomy (7–10).

In particular, neoadjuvant systemic therapy has been evaluated in multiple clinical trials as a primary intervention to reduce morbidity and mortality of prostate cancer in intermediate- and high-risk patients. These studies have focused on the intensification of ADT with more potent AR axis inhibitors. A recurrent outcome measure in these trials has been the determination of the pathologic complete response (pCR) rate, which implies the complete elimination of disease, although a threshold for specifying minimal residual disease (MRD) similarly identifies exceptional responders. In an exploratory pooled analysis of three neoadjuvant studies (11), neoadjuvant

[1]Genitourinary Malignancies Branch, Center for Cancer Research, NCI, NIH, Bethesda, Maryland. [2]Molecular Imaging Program, NCI, NIH, Bethesda, Maryland. [3]Laboratory for Genitourinary Cancer Pathogenesis, NCI, NIH, Bethesda, Maryland. [4]Division of Cancer Treatment and Diagnosis, Biometric Research Program, NCI, NIH, Rockville, Maryland. [5]Laboratory of Pathology, NCI, NIH, Bethesda, Maryland. [6]Clinical Research Directorate/Clinical Monitoring Research Program, Leidos Biomedical Research, Inc., NCI Campus at Frederick, Frederick, Maryland. [7]Department of Pathology, Brigham and Women's Hospital and Harvard Medical School, Boston, Massachusetts. [8]Department of Pathology, Ronald Reagan UCLA Medical Center, Los Angeles, California. [9]Urologic Oncology Branch, NCI, NIH, Bethesda, Maryland.

Note: Supplementary data for this article are available at Clinical Cancer Research Online (http://clincancerres.aacrjournals.org/).

F. Karzai and S.M. Walker contributed equally as co-first authors of this article.

P.A. Pinto and W.L. Dahut contributed equally as co-senior authors of this article.

ClinicalTrials.gov identifier: NCT02430480.

Corresponding Author: William L. Dahut, Center for Cancer Research, NCI, CRC 3-2571, 10 Center Drive, Bethesda, MD 20814. Phone: 301-222-3233; E-mail: dahutw@mail.nih.gov

Clin Cancer Res 2021;27:429–37

doi: 10.1158/1078-0432.CCR-20-2344

Translational Relevance

In high-risk localized prostate cancer, despite definitive therapy with either radical prostatectomy or radiotherapy plus androgen deprivation therapy (ADT), many patients will have recurrence of disease. Androgen receptor (AR) pathway inhibitors are increasingly being studied in men prior to prostatectomy. Studies suggest that intense ADT prior to prostatectomy may have a positive impact on time to biochemical recurrence. Incorporating imaging modalities, such as multiparametric MRI (mpMRI), to neoadjuvant AR-directed therapies may help with selection of patients who would benefit the most from this type of treatment. In this study, men with localized intermediate- or high-risk prostate cancer underwent a baseline mpMRI and mpMRI-targeted biopsy followed by a second mpMRI after 6 months of enzalutamide and ADT prior to robot-assisted radical prostatectomy. We found that low relative lesion volume at baseline mpMRI was predictive of pathologic response and may be a consideration when selecting patients for future neoadjuvant studies.

treatment prior to radical prostatectomy showed a positive impact on time to biochemical recurrence (BCR). Patients below the MRD threshold did not experience BCR in the timeframe of the meta-analysis, suggesting that complete response (CR) or MRD is a short-term surrogate outcome for BCR.

Utilizing intense ADT with enzalutamide in the neoadjuvant setting in combination with a dedicated imaging modality, such as multiparametric MRI (mpMRI), is a potentially promising strategy in high-risk localized disease. There is a critical need to incorporate newer imaging modalities to better define the initial tumor burden and subsequent response. While mpMRI has been successfully used to identify high-risk disease for sampling by biopsy (12), the role of mpMRI in the setting of neoadjuvant therapy is unclear. This feasibility trial was designed to evaluate tumors on mpMRI both before and after treatment with enzalutamide plus ADT prior to robot-assisted radical prostatectomy (RARP), and to correlate imaging findings with final pathology findings.

Patients and Methods

Study approval

This trial was approved by the Institutional Review Board of the Center for Cancer Research, NCI (Bethesda, MD; ClinicalTrials.gov identifier: NCT02430480). This study has been conducted in accordance with ethical principles that have their origin in the Declaration of Helsinki and are consistent with the International Council on Harmonisation guidelines on Good Clinical Practice, all applicable laws and regulatory requirements, and all conditions required by a regulatory authority and/or institutional review board. Written informed consent was obtained from all patients prior to performing study-related procedures in accordance with federal and institutional guidelines.

Study design

In this study, men with newly diagnosed intermediate- or high-risk localized prostate cancer were treated for 6 months with complete androgen blockade with enzalutamide, a potent AR antagonist, plus ADT with goserelin, leuprolide, or degarelix (based on discretion of the treating physician), followed by RARP. Patients underwent two mpMRIs, one at baseline and one after 6 months of treatment. Each patient underwent subsequent RARP with whole-mount histopathologic analysis to assess lesion response.

Eligible patents had pathologically confirmed intermediate- or high-risk localized prostate cancer with no prior history of treatment for prostate cancer. Intermediate-risk disease was defined as a PSA level of 10–20 ng/mL or a Gleason score of 7 or clinical stage T2b or T2c. High-risk disease was defined as PSA > 20 ng/mL at diagnosis or Gleason score of 8–10 or seminal vesicle involvement or possible extracapsular extension (on mpMRI). Patients were required to have an Eastern Cooperative Oncology Group performance status of 0–1 and baseline testosterone levels of ≥100 ng/dL. Patients with distant metastatic disease beyond N1 (regional) lymph nodes on conventional imaging studies (CT, MRI, or bone scan) were excluded.

This was an open-label feasibility study of enzalutamide 160 mg orally daily × 28 days for a total of six cycles plus ADT. Thirty-seven patients received goserelin 10.8 mg subcutaneously at week 0 and week 12 on-treatment. One patient had leuprolide acetate depot 22.5 mg intramuscularly × two doses. One patient received the loading dose of degarelix (240 mg subcutaneously at week 0), followed by degarelix 80 mg subcutaneously × one dose at week 4 and was transitioned to goserelin at week 8. Patients underwent two separate mpMRIs of the prostate, at baseline and after 24 weeks, followed by RARP (**Fig. 1**). Patients who underwent MRI-targeted combined biopsy at the NCI (Bethesda, MD) for prostate cancer diagnosis did not require an additional biopsy prior to study enrollment. If a patient had not undergone an MRI-targeted biopsy previously, a second biopsy was required.

Surgery and pathologic analysis

Initial pathology was determined by transrectal ultrasound (TRUS)-guided systematic biopsy, if there was reasonable assurance that the biopsy was from the index lesion, and/or TRUS-MRI fusion-guided biopsy prior to initiation of neoadjuvant enzalutamide plus ADT. The index lesion by mpMRI was defined as the lesion with the largest size and highest Prostate Imaging Reporting and Data Systems (PI-RADS)

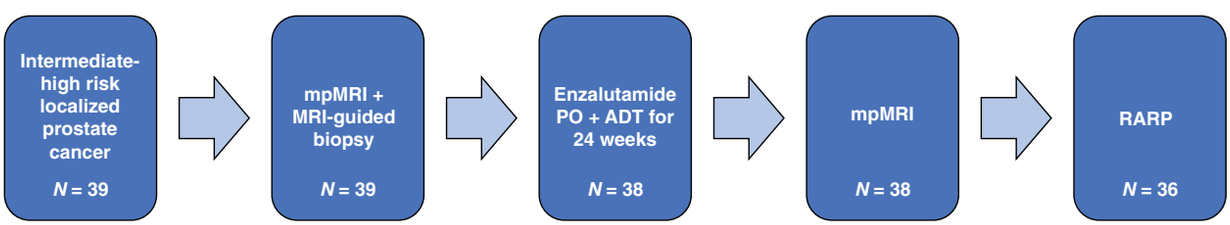

Figure 1.
Study schema.

score. All biopsy specimens were reviewed and assigned Gleason scores by a genitourinary pathologist.

RARP was performed on 36 patients after 24 weeks of complete androgen blockade and final mpMRI. A single urologist performed all, but one, RARP. All patients underwent extended lymph node dissection. Whole-mount prostate pathology slides were prepared using 3D-printed custom prostate molds to correspond with slices from each patient's final mpMRI scan (13).

All posttreatment specimens were analyzed by two nonblinded genitourinary pathologists. Postoperative pathologic staging was assigned to each patient; however, Gleason tumor grade could not be assigned to residual tumors due to treatment effect. Presence of residual tumor was noted and annotated on hematoxylin and eosin whole-mount pathology slides. For 3 patients who demonstrated substantial pathologic resistance to treatment, the NCI Laboratory of Pathology selected formalin-fixed, paraffin-embedded tissue blocks for panel-based Oncomine Comprehensive Assay v3 (Thermo Fisher Scientific) sequencing to determine potential eligibility for ongoing clinical trials.

Image analysis of mpMRI

Prostate and lesion volumes on baseline and posttreatment mpMRIs were calculated from T2W-MRI sequences using software embedded in the PACS after manual contouring by the same radiologist (B. Turkbey). mpMRIs at baseline and after 24 weeks of neoadjuvant treatment were acquired with a 3-Tesla Scanner (Achieva; Philips Healthcare). Patients underwent imaging with integrated external (surface) phased array coil and endorectal coil. Imaging studies were interpreted by a single genitourinary radiologist with over 10 years of experience in prostate imaging. Evaluated imaging sequences included T2W-MRI, apparent diffusion coefficient (ADC) maps of diffusion-weighted imaging, high b value ($b = 2{,}000$ seconds/mm^2), and dynamic contrast-enhanced MRI (temporal resolution = 5.6 seconds). Lesions at baseline mpMRI were assigned PI-RADS categories based on stringent interpretation of PI-RADSv2.0 guidelines (ref. 14; PI-RADSv2.1 was published near the end of this study).

All MRI visible lesions at baseline were documented and followed over the course of the study. Evidence of extraprostatic extension (EPE), seminal vesical invasion, and bulky nodal disease was noted in mpMRI reports. Each mpMRI scan was assigned an EPE grade from 0 to 3, as described previously (15): 0, no evidence of EPE; 1, large lesion-capsule contact length or capsular bulge; 2, large lesion-capsule contact length and capsular bulge; and 3, frank EPE. Only EPE grade 0 was considered "organ-confined disease." Per PI-RADSv2 guidelines, up to four MRI visible lesions per patient were targeted for biopsy and were included in lesion-level analyses, irrespective of biopsy Gleason score. Biopsy targeting was performed using a commercially available TRUS/MRI-fusion Biopsy Platform, UroNav (InVivo, Philips). Prior to biopsy, whole prostate gland MRI and MRI visible lesions were manually segmented using the DynaCad Platform (InVivo).

In addition to these qualitative mpMRI characteristics, higher order quantitative metrics were obtained from baseline mpMRI scans, including lesion volume, ADCs, and perfusion (Ktrans; calculated using a two-compartment Tofts model with standardized arterial input function). In patients with multiple contoured lesions at baseline, their volumes were added to produce a patient-level mpMRI lesion volume. To assess MRI evidence of neoadjuvant treatment response, post-treatment mpMRI scans were acquired with the same parameters; however, PI-RADS categories were not assigned because of treatment effects on MRI. On both mpMRI scans, total prostate volume was measured. Relative tumor burden (RTB) volumes were calculated by dividing the combined volumes of each lesion by the prostate volume, such that RTB is expressed as the percentage of prostate volume taken by the tumor.

Residual cancer burden calculations

Residual tumor was concordantly identified by three board-certified genitourinary pathologists (M.J. Merino, R.T. Lis, and H. Ye). Pathologic analysis was performed independently from imaging analysis, and pathologists did not have access to imaging data to inform tissue analysis. All prostate specimens were completely submitted for identification of residual disease. Residual cancer burden (RCB) was measured and calculated by multiplying the number of slices through which each residual tumor extended by the largest cross-sectional width and length and block thickness (0.6 cm). Volume was further corrected by multiplying by 0.4 and the estimated tumor cellularity. MRD was considered <0.05 cc, and nonresponse (NR) was >0.05 cc. Each mpMRI visible lesion was similarly classified on the basis of the volume of the evaluable tumor remaining in the anatomic region the lesion was in. If a patient had more than one residual lesion at final pathology, the largest cross-sectional dimension of tumor was used to determine RCB for the purpose of classifying the patient as MRD or NR.

Statistics on mpMRI

Logistic regression analysis was performed to correlate clinical variables and MRI parameters, with patient response categorized as CR/MRD versus NR. Variables which were significant at the 0.05 level in the univariable analysis were considered for multivariable analysis. The performance of predictors was evaluated by the AUC with its 95% confidence interval determined by the Delong method. The Youden index was calculated to determine the cutoffs that gave the optimal combination of sensitivity and specificity for patient response. A two-sided $P < 0.05$ was considered statistically significant for all analyses. All analyses were conducted using R 3.6.1 (R Foundation for Statistical Computing).

Results

Between June 2015 and September 2018, 39 patients with newly diagnosed localized prostate cancer were enrolled on this study and treated with enzalutamide plus ADT (see **Fig. 1**). The median baseline PSA was 9.56 ng/mL (1.18–985.9 ng/mL). The median grade group was 4 (Gleason score 8). Thirty-six patients had high-risk disease and 3 had intermediate-risk disease (**Table 1**). Three patients did not complete RARP. One patient died from a recreational drug overdose during the first month of treatment. A second patient was unable to undergo RARP due to anesthesia concerns, and 1 patient progressed on-treatment. A third patient exhibited tumor extension to the bladder while on treatment and underwent palliative transurethral resection of the prostate/transurethral resection of a bladder tumor (TURP/TURBT) due to the extent of the prostate cancer, and, thus, did not underwent RARP, so final pathology volumes were not available. He went on to receive radiotherapy to the pelvis.

Of 39 patients enrolled on-study, 3 had disease progression with enlargement of lesions on mpMRI (**Fig. 2A**). All three nonresponders recurred during the first year. One patient progressed during treatment (as above) and 2 progressed shortly after RARP. In addition, to date, 9 patients had recurred biochemically; 2 patients in the first year, 5 patients in the second year, and 2 patients during the third year. The

Table 1. Baseline patient characteristics for 39 patients with localized prostate cancer.

Demographics		
	Year	(IQR)
Median age	61	(58–69)
Race	%	(*N*)
White	69	(27)
Black	15	(6)
Other	15	(6)
Clinical		
	#	(IQR)
Median PSA (ng/mL)	9.56	(1.18–985.9)
Median PSA density	0.22	(0.15–0.39)
Median prostate volume (cc)	42.0	(33.0–49.0)
Median MRI tumor burden (cc)	3.47	(1.9–9.8)
Risk group	%	(*N*)
Intermediate	8	3
High	92	36
Histology		
Pathologic stage	%	(*N*)
T2	15	(6)
T3a	44	(17)
T3b	28	(11)
T4	12	(5)
N1	28	(11)
Gleason score (grade group)	%	(*N*)
3 + 4 (2)	15.4	(6)
4 + 3 (3)	12.8	(5)
4 + 4 (4)	28.2	(11)
4 + 5; 5 + 4; 5 + 5 (5)	46.6	(17)

Note: Data are presented as *N* (IQR) or % (*N*).
Abbreviation: IQR: interquartile range.

median follow-up was 3 years. Two of the nonresponders went on to develop metastatic disease and 1 has died.

Adverse events

Treatment was well-tolerated, with no grade 4 events and one grade 5 event not attributable to study treatment (Supplementary Table S1). The most common adverse events were grade 1 hot flashes (34/39, 87%), grade 1 fatigue (20/39, 51%), grade 1 decrease in libido (15/39, 38%), grade 1 insomnia (12/39, 31%), and grade 1 erectile dysfunction (9/39, 23%). Grade 2 and grade 3 hypertension (18% each) was manageable with effective antihypertensive medication. No patients discontinued therapy because of toxicity. Sexual function assessment was captured through the Common Terminology Criteria for Adverse Events and not through sexual function assessment.

Response to neoadjuvant treatment on mpMRI

Within the study population, 59 lesions were detected at baseline mpMRI and 40 remained measurable at follow-up mpMRIs after 24 weeks of enzalutamide plus ADT. Fifty-five of 59 lesions (93%) demonstrated greater than 50% volume reduction on posttreatment mpMRI. Three of 59 lesions (5%) demonstrated growth in size at follow-up imaging, with two of the lesions increasing more than 3-fold in volume (**Fig. 2A**). At baseline mpMRI, all patients had measurable disease, with a median tumor burden of 3.44 cc. Median prostate volume decreased from 39.5 to 20 cc after treatment, and median PSA decreased from 9.56 ng/mL to undetectable (<0.02 ng/mL). On posttreatment MRI, 4 of 36 patients (11%) had no visible disease, and on final pathology, 2 of 36 patients (6%) were staged as a complete pathologic response (ypT0N0). Six of 36 patients (17%) had no evidence of EPE on baseline mpMRI, and this number increased to 21 patients (58%) without EPE at mpMRI after treatment. Twenty-three patients (64%) had organ-confined disease on final pathology. On baseline mpMRI, 4 patients (11%) had evidence of bladder or rectal invasion; only 1 patient had visible bladder or rectal invasion on follow-up imaging and on final pathology. **Table 2** summarizes mpMRI evidence of pathologic features before and after treatment, including EPE, SVI lymph node involvement, etc., and corresponding findings at final pathology.

Upon final pathologic analysis, nine lesions (15%) demonstrated CR, 30 lesions (52%) demonstrated MRD, and 19 lesions (33%) demonstrated NR (**Fig. 2A**). At the patient level, 2 patients (6%) demonstrated CR, 13 patients (36%) demonstrated MRD, and 22 patients (61%) demonstrated NR, including 1 patient who underwent TURP/TURBT for prostate cancer (**Fig. 2B**). Two patients with NR were determined by IHC of posttreatment tissue to have decreased AR and PSA expression in combination for positive staining for synaptophysin and Ki-67, which indicated

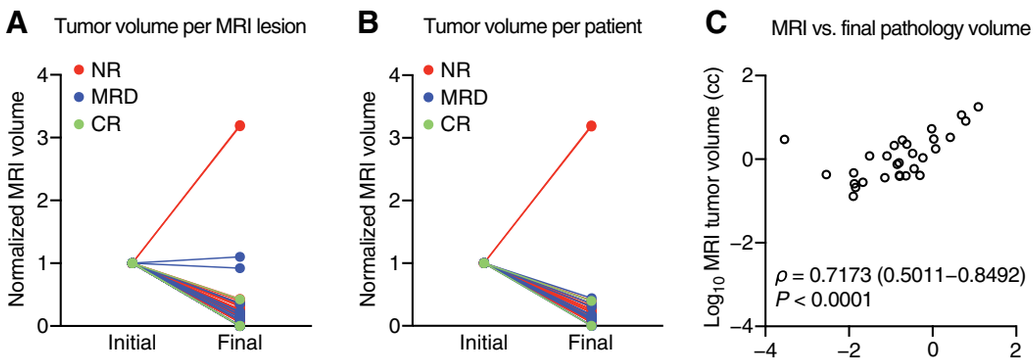

Figure 2.
Response to neoadjuvant enzalutamide plus ADT. **A,** Fifty-five of 59 lesions demonstrated >50% volume reduction. **B,** Thirty-six of 38 patients demonstrated >50% volume reduction. Lesions and patients are color coded on the basis of pathologic response to treatment at radical prostatectomy. One patient completed baseline and post-enzalutamide plus ADT mpMRI, but did not undergo RARP, thus he was included to demonstrate MRI evidence of extreme NR, but was excluded from all analyses involving pathologic response to treatment. **C,** Spearman correlation of final imaging volumes per patient with final pathologic RCB, logarithmically transformed. Values of zero were transformed to nominal values to preserve their rank within the dataset, but omitted from the graph.

Table 2. mpMRI detection of pathologic features before and after complete androgen blockage and corresponding findings on whole-mount RARP specimens ($N = 36$).

Feature	Baseline	Posttreatment	Final pathology
No visible disease	0 (0%)	4 (11%)	2 (6%)
Organ-confined disease	6 (17%)	21 (58%)	23 (64%)
Seminal vesical invasion	10 (28%)	6 (17%)	8 (22%)
Regional lymph node involvement	10 (28%)	7 (19%)	5 (14%)
Bladder/rectal invasion	4 (11%)	1 (3%)	1 (3%)

neuroendocrine differentiation (16, 17). The combined volumes of each imaging lesion per patient demonstrated a statistically significant correlation with final pathology RCBs with Spearman $\rho = 0.7173$ (**Fig. 2C**).

For the 3 NR patients (Supplementary Table S3) who demonstrated substantial volumes of residual disease or progression on treatment, we performed clinical cancer panel sequencing on posttreatment surgical tissue using the Oncomine platform to assess potential drivers and determine eligibility for additional trials. Germline alterations to homologous recombination genes were observed in 2 of the 3 patients (*BRCA2* frameshift and *PALB2* nonsense), with loss-of-function alterations to *RB1* observed in all three cases. In 1 patient whose radical prostatectomy specimen demonstrated focal neuroendocrine features, biallelic inactivation of *TP53, PTEN*, and *RB1* was observed in conjunction with the *TMPRSS2-ERG* fusion.

Pathology and IHC results

As enzalutamide plus ADT synergize by reducing the concentration of testosterone, dihydrotestosterone, and androgens binding to the AR, the effect of intense androgen suppression and inhibition was measured on tumors using anti-AR and anti-PSA immunostains of biopsy and surgical specimens (**Fig. 3A** and **B**). Median nuclear AR levels were substantially higher in diagnostic biopsy specimens versus residual tumor (staining indices of 0.7568 and 0.1661, respectively, $P < 0.0001$ by Welch t test; **Fig. 3C**). As the *KLK3* gene, encoding the PSA protein, is a primary target of AR-driven transcription, anti-PSA IHC was performed to assess AR activity *in situ*. Like AR, median cytoplasmic PSA histology scores of residual tumors were substantially lower compared with pretreatment tumor biopsies (0.1380 and 0.7062, respectively, $P < 0.0001$ by Welch t test), demonstrating reduced, but persistent AR activity (**Fig. 3D**).

TMPRSS2-ERG fusion occurs in approximately 50% of prostate cancers and frequently cooccurs with the loss of *PTEN*, which, in turn, is associated with more aggressive prostate cancer (18). Therefore, ERG protein overexpression and *PTEN* reduction were evaluated using IHC in posttreatment specimens (**Fig. 3E**). Of 37 patients who completed treatment and underwent surgery, evaluable residual tumor was available in 32 cases, of which 14 (43.8%) harbored ERG-positive tumor cells and 21 (65.6%) demonstrated *PTEN* staining reduction or loss (**Fig. 3F**). Comparing pCR/MRD versus NR cases, reduction of *PTEN* showed significant differences ($P = 0.0006$, Fisher exact test) between the pCR/MRD group (two cases, 20%) versus the NR group (19 cases, 86.4%). However, the difference between groups was less with respect to ERG-positive tumor cell staining (20% vs. 54.5%, respectively; $P = 0.073$, Fisher exact test) and the combined reduction of *PTEN* with ERG-positive staining (8.3% vs. 50%, respectively; $P = 0.0931$, Fisher exact test). Therefore, reduction of *PTEN* levels is significantly associated with resistance to intense ADT driving greater residual tumor volumes.

Predicting patient-level response from baseline imaging

Although final imaging volumes correlated well with RCBs (see **Fig. 1C**), we performed extensive univariate analyses on baseline imaging features to determine whether final pathologic response could be predicted by mpMRI. Patient-level imaging characteristics associated with patient-level treatment response are listed in Supplementary Table S3. As depicted in **Fig. 4A**, low RTB (i.e., the combined volume of each tumor lesion divided by the total prostate volume) was the only predictor in the final multivariate logistic regression model [OR, 0.77 (0.63–0.94); $P = 0.001$]. **Figure 4B** shows that the AUC for RTB was 0.89 (0.79–0.99) at the optimal cutoff of 8.1% for RTB specificity (81%) and sensitivity (87%). Representative responder and nonresponder cases are shown in **Fig. 4C**, which were both high-risk, cT3a cases. The responder initial lesion volume was 1.56 cc, so with a baseline prostate volume of 46 cc, the RTB was 3.39%. In contrast, the nonresponder lesion volume was 7.13 cc at the start of treatment, and with a baseline prostate volume of 33 cc, the RTB was 21.6%.

Discussion

The effects of neoadjuvant therapies on prostate tumors are not uniform among patients or even in distinct cancer lesions within a patient's prostate (19). Information from mpMRI of the prostate after intense androgen deprivation can be used to assess treatment response on a per-lesion and per-patient basis, as well as for surgical planning. Predicting which patients will respond to neoadjuvant therapies based on baseline mpMRI characteristics could allow for better patient selection and overall responses to treatment in subsequent clinical trials, while patients who would not benefit from treatment would be spared from toxicities (20). mpMRI may also be able to identify patients with intrinsic resistance despite declines in PSA. This intrinsic resistance, as seen with androgen independence leading to tumor cell lineage plasticity, may play a role in resistance to AR-targeted therapy (21). Thus, perturbations in AR-regulated lineage characteristics observed phenotypically by less PSA expression and genomic loss of tumor suppressors, such as *RB1* and *TP53*, may represent aggressive prostate variants. Early identification of this high-risk population, aided by imaging, is paramount to treatment of this subset of patients.

We found that low RTB on mpMRI was the best predictor of response and was the only baseline characteristic that showed statistically significant predictive performance in multivariate analysis at both the lesion and patient levels. This was the strongest predictor of pathologic response, with an optimal cutoff of 8.1%, and may be a consideration when selecting patients for future neoadjuvant studies. Contouring of the prostate and lesions within the prostate on mpMRI to obtain a volume can be performed by radiologists with readily available software, and automated lesion segmentation software is becoming available. This makes baseline mpMRI an important prognostic tool for predicting tumor- and patient-level response to neoadjuvant intense ADT.

Posttreatment mpMRI revealed a significant decrease in tumor volume after therapy in an overwhelming majority of patients, although at baseline and after 6 months of treatment, it is not possible to determine the kinetics of tumor reduction during treatment. It is important to note that while 4 of 36 patients had no visible disease on mpMRI, on final pathology only 2 of 36 patients had complete pathologic response. However, studies suggest lesions undetected by

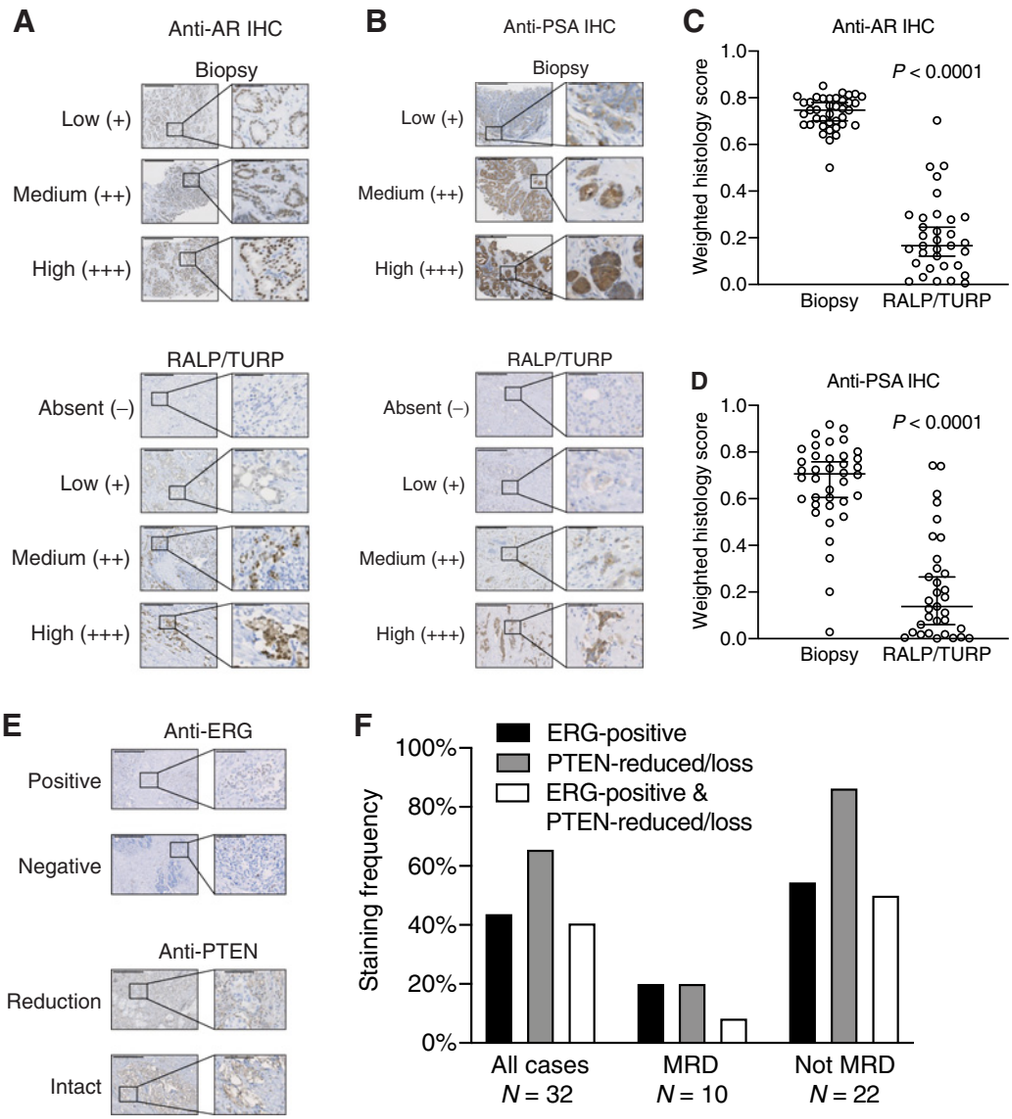

Figure 3.

Histologic analysis of *in situ* tissue phenotypes. Representative micrographs of low, medium, and high histology scores for anti-AR (**A**) and anti-PSA (**B**) immunostaining of biopsies (top) and absent, low, medium, and high histology scores for posttreatment surgical RALP or TURP specimens (bottom). There were no examples of absent anti-AR or PSA staining in pretreatment biopsied tumor tissue. Scale bar, 500 μm. Inset scale bar, 100 μm. Tissue sections immunostained with anti-AR from biopsies ($N = 39$ cases representing 82 different tissue blocks) and posttreatment surgical specimens ($N = 33$ cases representing 61 different tissue blocks; **C**) or anti-PSA from biopsies ($N = 38$ cases representing 79 different tissue blocks) and posttreatment surgical specimens ($N = 33$ cases representing 64 different tissue blocks; **D**) were quantified with Definiens to measure stain intensity. Histology scores were reported on a weighted index of 0 to 1, and multiple slides from the same individual were added before computing the index. Each circle represents a single patient. Bars represent median and 95% confidence interval. $P < 0.0001$ for both AR and PSA staining, by Welch *t* test. **E,** Representative micrographs of positive (overexpressed) and negative nuclear ERG immunostaining (left) and reduced or intact PTEN (right) in posttreatment tissue. Scale bar, 500 μm. Inset scale bar, 100 μm. Note that nuclear ERG intensity is reduced relative to endogenous ERG expression in endothelial cells on account of its expression being driven by (reduced) AR activity. **F,** Posttreatment tissue sections were immunostained with anti-ERG and anti-PTEN antibodies and the frequency of ERG-positive tumor cells (any percentage positive), or PTEN-reduced or PTEN-deficient (at least 5% of tumor cells) cells is shown. pCR/MRD versus NR for PTEN was different at $P = 0.0006$ by Fisher exact test.

mpMRI may be lower in grade and size than detected lesions, making mpMRI an important tool in risk-stratifying prostate cancer (22). Nonetheless, among all patients, the residual cancer volumes estimated by posttreatment mpMRI correlated well with final pathology at $\rho = 0.7173$, making the serial mpMRI a meaningful measure for assessing organ-wide response when comprehensive pathologic analyses are not routinely feasible.

Previous studies have demonstrated that the positive staining for the *TMPRSS2-ERG* fusion and *PTEN* loss by IHC is enriched in patients with increased volumes of residual disease (8, 23). We similarly observed that NR patients exhibited increased rates of positive ERG staining and negative *PTEN* staining than CR/MRD, although only *PTEN* reduction was statistically significant ($P = 0.0006$). In 3 patients who demonstrated minimal tumor reductions on posttreatment

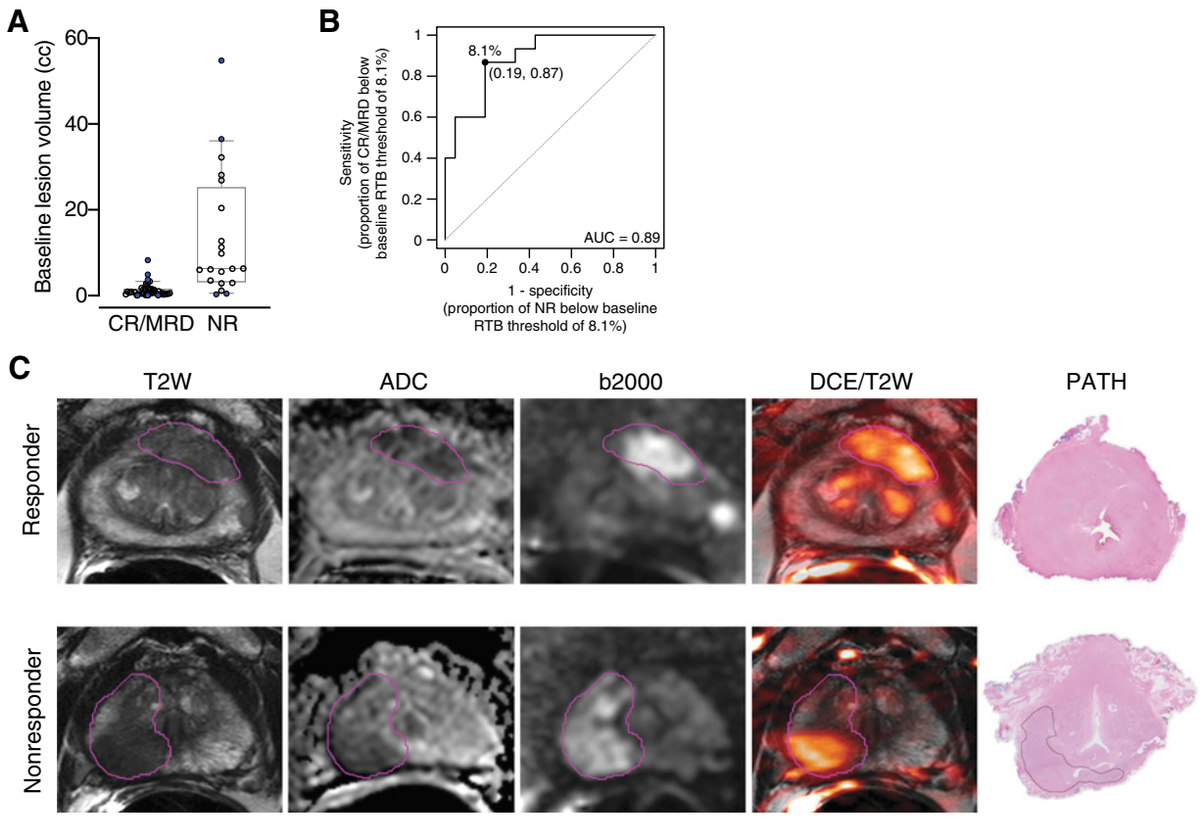

Figure 4.

Low RTB is a statistically significant predictor of final pathologic outcome. **A,** Baseline lesion volumes in cc, based on the final pathology status for each patient. $N = 39$ for CR/MRD lesions and $N = 20$ for NR lesions. $P < 0.001$ by two-sided Mann–Whitney test. **B,** ROC curve for pretreatment RTB yielding an AUC of 0.89 and optimal threshold of 8.1%. **C,** Baseline mpMRIs of 2 different patients with high-risk localized prostate cancer and corresponding final pathology. Responder, 72-year-old with a PSA of 5.81 ng/mL had a PI-RADS 5 lesion in the left apical-mid anterior peripheral zone which revealed Gleason 4+4 = 8 cancer at targeted biopsy. Baseline RTB was 3.4% of the prostate. Final pathology revealed pCR. Nonresponder, 66-year-old with a PSA of 5.53 ng/mL, had a large PI-RADS 5 lesion in the right apical-base peripheral zone which revealed Gleason 4+5 = 9 cancer at targeted biopsy. Baseline RTB was 21.5% of the prostate. Final pathology revealed the patient was a nonresponder with RCB of 0.24 cc.

mpMRI, we performed additional genomic analysis to assess eligibility for biomarker-driven studies; in particular, loss of homologous recombination genes would indicate eligibility for treatment with olaparib. In 2 of these 3 patients, germline pathologic variants to *BRCA2* and *PALB2* were observed. Interestingly, one- or two-copy loss of *RB1* was found in all 3 patients, and biallelic inactivation of *TP53* was also observed in 2 patients. Although these findings are anecdotal, they emphasize the consequence of bypassing the AR via *RB1* loss (often in conjunction with loss of tumor suppressors or due to a defect in DNA damage response). As these genomic events are more frequently associated with the "AR low" phenotypes of localized prostate cancer (23), it aligns with our finding that the vast majority of all posttreatment specimens expressed less AR and PSA despite variable volumes of residual disease. Because AR indifference, including neuroendocrine transdifferentiation (24), can result from treatment with AR axis inhibitors, like enzalutamide and abiraterone, the use of genomic analysis to infer resistance mechanisms is needed in the neoadjuvant setting. Furthermore, earlier evaluation with imaging and molecular characteristics might better predict resistance, enabling discontinuation in patients unlikely to benefit from neoadjuvant therapy.

The results of our study reveal a significant increase in the number of patients with organ-confined disease at imaging prior to RARP. It has been suggested that patients receiving neoadjuvant ADT prior to radical prostatectomy are more likely to have negative surgical margins at radical prostatectomy (25, 26). The effect of negative margins on BCR has not been well characterized in patients who undergo neoadjuvant ADT prior to surgery, and some studies have described a lack of significant decreases in rates of BCR in this population compared with those who undergo radical prostatectomy alone (27, 28). While this study and other similar phase II studies have shown favorable imaging and pathologic responses to neoadjuvant AR antagonists plus ADT in patients with high-risk localized disease, long-term follow-up for overall survival needs to be considered (8, 29).

There are several limitations to this study. First, a small sample size of 36 patients limits the power of our statistical analyses. Second, all mpMRI scans were interpreted and contoured by a single radiologist who specializes in prostate mpMRI, which could limit reproducibility of results. However, new lesion-segmenting software may soon mitigate this problem. Third, mpMRIs were acquired using an endorectal coil, which may have influenced the results. Most mpMRIs are increasingly obtained without an endorectal coil. However, the

endorectal coil was used here to ensure the highest quality images. Fourth, although clinical grade Oncomine sequencing identified 3 patients with RB loss, only 1 of these utilized a pretreatment biopsy sample, and were not confirmed using anti-RB IHC on any of the specimens. Finally, the short-term follow-up of this study precludes using time to BCR as an outcome to assess neoadjuvant intense ADT. However, the finding that low residual tumor volumes (i.e., CR and MRD) were associated with freedom from BCR (11) implies that the 15 patients in our study who exhibited CR/MRD are less likely to experience BCR within 3 years than the 22 patients who did not.

To our knowledge, this is one of the first studies to combine serial mpMRI imaging with neoadjuvant intense ADT in prostate cancer. On the basis of our findings, imaging with mpMRI may enhance patient selection for neoadjuvant treatment. Although most (but not all) of patients with the RTB had CR/MRD, nearly every patient experienced tumor shrinkage regardless of initial tumor burden, and this finding was consistent with previous neoadjuvant intense ADT studies (8–10). Thus, patients with higher RTBs at baseline were less likely to benefit from the regimen in this study, they might benefit from either a longer duration of intense ADT or an alternative or precision-guided treatment, with such decision being guided by a combination of clinical, pathology, and imaging assessments. Neoadjuvant treatment in our patient population was tolerable, and extension of treatment beyond 6 months may be feasible.

Neoadjuvant enzalutamide with ADT prior to RARP significantly reduces tumor burden at mpMRI in most patients with localized high-risk prostate cancer. Baseline low RTB at mpMRI was the strongest predictor of pathologic response, with an optimal cutoff of 8.1%, a consideration when selecting patients for future neoadjuvant studies. In addition, imaging can enhance evaluation for high-risk molecular signatures, where combination with imaging can be used to identify patients who are unlikely to benefit from intensive neoadjuvant ADT. In this study, we found mpMRI can be used to assess treatment responses, and 3 patients with adverse pathologic features and multiple deleterious genomic alterations also experienced RCB. Deeper molecular analysis of this and other neoadjuvant studies [i.e., ClinicalTrials.gov identifier NCT03860987 involves mpMRI at mid-treatment along with 18F-DCFPyL (PSMA) imaging] will facilitate patient selection and development of appropriate endpoints for neoadjuvant therapies in prostate cancer.

Authors' Disclosures

D.J. VanderWeele reports other from Genzyme and personal fees from Clovis outside the submitted work. M. Bilusic reports employment with NCI. R.T. Lis reports personal fees from Janssen outside the submitted work. H. Ye reports personal fees from Janssen Pharmaceuticals (Johnson & Johnson) outside the submitted work. P.L. Choyke reports being an inventor of a method of MRI-ultrasound fusion biopsy that was used in the study; this invention is patented by the U.S. Government and licensed to Philips Medical Systems that has commercialized the method as "UraNav", however, this is not directly related to this study. A.G. Sowalsky reports grants from U.S. Department of Defense during the conduct of the study. B. Turkbey reports other from Cooperative (research and development agreements with Philips and Nvidia), royalties from InVivo, and a patent for related intellectual property in field of prostate computer-aided diagnosis (NIH owned) outside the submitted work. P.A. Pinto reports other from Philips/InVivo Inc during the conduct of the study and outside the submitted work, and has a patent 8,447,384 issued and with royalties paid from Philips/InVivo Inc and a patent for 10,215,830 issued and with royalties paid from Philips/InVivo Inc. No disclosures were reported by the other authors.

Disclaimer

The content of this article does not necessarily reflect the views or policies of the Department of Health and Human Services or the Department of Defense, nor does mention of trade names, commercial products, or organizations imply endorsement by the U.S. Government.

Authors' Contributions

F. Karzai: Conceptualization, data curation, formal analysis, investigation, writing-original draft, writing-review and editing. **S.M. Walker:** Data curation, formal analysis, investigation, writing-original draft, writing-review and editing. **S. Wilkinson:** Data curation, investigation, methodology. **R.A. Madan:** Conceptualization, data curation, investigation, methodology, writing-review and editing. **J.H. Shih:** Formal analysis, writing-review and editing. **M.J. Merino:** Data curation, formal analysis, investigation. **S.A. Harmon:** Formal analysis. **D.J. VanderWeele:** Data curation, formal analysis, writing-review and editing. **L.M. Cordes:** Investigation, writing-review and editing. **N.V. Carrabba:** Data curation, writing-review and editing. **J.R. Bright:** Data curation, methodology, writing-review and editing. **N.T. Terrigino:** Data curation, methodology, writing-review and editing. **G. Chun:** Investigation, writing-review and editing. **M. Bilusic:** Investigation, writing-review and editing. **A. Couvillon:** Investigation, writing-review and editing. **A. Hankin:** Investigation, writing-review and editing. **M.N. Williams:** Investigation, writing-review and editing. **R.T. Lis:** Investigation, writing-review and editing. **H. Ye:** Data curation, formal analysis, writing-review and editing. **P.L. Choyke:** Data curation, software, formal analysis, investigation, writing-review and editing. **J.L. Gulley:** Investigation, writing-review and editing. **A.G. Sowalsky:** Data curation, formal analysis, writing-review and editing. **B. Turkbey:** Data curation, software, formal analysis, writing-review and editing. **P.A. Pinto:** Data curation, investigation, writing-review and editing. **W.L. Dahut:** Conceptualization, data curation, formal analysis, investigation, writing-review and editing.

Acknowledgments

The authors thank all the patients who participated in this study and their families. Enzalutamide, goserelin, leuprolide acetate, and degarelix were provided through the Center for Cancer Research, NIH. This project was supported by the Prostate Cancer Foundation (Young Investigator Awards to F. Karzai, S. Wilkinson, R.A. Madan, S.A. Harmon, D.J. VanderWeele, H. Ye, and A.G. Sowalsky), the Department of Defense Prostate Cancer Research Program (W81XWH-19-1-0712 to S. Wilkinson and W81XWH-16-1-0433 to A.G. Sowalsky), the NCI (HHSN261200800001E), and the Intramural Research Program of the NCI, NIH. The authors also thank Bonnie L. Casey for editorial assistance in the preparation of this article.

The costs of publication of this article were defrayed in part by the payment of page charges. This article must therefore be hereby marked *advertisement* in accordance with 18 U.S.C. Section 1734 solely to indicate this fact.

Received June 16, 2020; revised August 26, 2020; accepted October 1, 2020; published first October 6, 2020.

References

1. Siegel RL, Miller KD, Jemal A. Cancer statistics, 2020. CA Cancer J Clin 2020;70:7–30.
2. Zelefsky MJ, Eastham JA, Cronin AM, Fuks Z, Zhang Z, Yamada Y, et al. Metastasis after radical prostatectomy or external beam radiotherapy for patients with clinically localized prostate cancer: a comparison of clinical cohorts adjusted for case mix. J Clin Oncol 2010;28:1508–13.
3. Scher HI, Fizazi K, Saad F, Taplin ME, Sternberg CN, Miller K, et al. Increased survival with enzalutamide in prostate cancer after chemotherapy. N Engl J Med 2012;367:1187–97.
4. Beer TM, Armstrong AJ, Rathkopf DE, Loriot Y, Sternberg CN, Higano CS, et al. Enzalutamide in metastatic prostate cancer before chemotherapy. N Engl J Med 2014;371:424–33.

5. Armstrong AJ, Szmulewitz RZ, Petrylak DP, Holzbeierlein J, Villers A, Azad A, et al. ARCHES: a randomized, phase III study of androgen deprivation therapy with enzalutamide or placebo in men with metastatic hormone-sensitive prostate cancer. J Clin Oncol 2019;37:2974–86.
6. Hussain M, Fizazi K, Saad F, Rathenborg P, Shore N, Ferreira U, et al. Enzalutamide in men with nonmetastatic, castration-resistant prostate cancer. N Engl J Med 2018;378:2465–74.
7. Aoun F, Bourgi A, Ayoub E, El Rassy E, van Velthoven R, Peltier A. Androgen deprivation therapy in the treatment of locally advanced, nonmetastatic prostate cancer: practical experience and a review of the clinical trial evidence. Ther Adv Urol 2017;9:73–80.
8. McKay RR, Ye H, Xie W, Lis R, Calagua C, Zhang Z, et al. Evaluation of intense androgen deprivation before prostatectomy: a randomized phase II trial of enzalutamide and leuprolide with or without abiraterone. J Clin Oncol 2019;37:923–31.
9. Montgomery B, Tretiakova MS, Joshua AM, Gleave ME, Fleshner N, Bubley GJ, et al. Neoadjuvant enzalutamide prior to prostatectomy. Clin Cancer Res 2017;23:2169–76.
10. Taplin ME, Montgomery B, Logothetis CJ, Bubley GJ, Richie JP, Dalkin BL, et al. Intense androgen-deprivation therapy with abiraterone acetate plus leuprolide acetate in patients with localized high-risk prostate cancer: results of a randomized phase II neoadjuvant study. J Clin Oncol 2014;32:3705–15.
11. McKay RR, Montgomery B, Xie W, Zhang Z, Bubley GJ, Lin DW, et al. Post prostatectomy outcomes of patients with high-risk prostate cancer treated with neoadjuvant androgen blockade. Prostate Cancer Prostatic Dis 2018;21:364–72.
12. Ahdoot M, Wilbur AR, Reese SE, Lebastchi AH, Mehralivand S, Gomella PT, et al. MRI-targeted, systematic, and combined biopsy for prostate cancer diagnosis. N Engl J Med 2020;382:917–28.
13. Turkbey B, Mani H, Shah V, Rastinehad AR, Bernardo M, Pohida T, et al. Multiparametric 3T prostate magnetic resonance imaging to detect cancer: histopathological correlation using prostatectomy specimens processed in customized magnetic resonance imaging based molds. J Urol 2011;186:1818–24.
14. Weinreb JC, Barentsz JO, Choyke PL, Cornud F, Haider MA, Macura KJ, et al. PI-RADS prostate imaging - reporting and data system: 2015, version 2. Eur Urol 2016;69:16–40.
15. Mehralivand S, Shih JH, Harmon S, Smith C, Bloom J, Czarniecki M, et al. A grading system for the assessment of risk of extraprostatic extension of prostate cancer at multiparametric MRI. Radiology 2019;290:709–19.
16. Wiedenmann B, Franke WW, Kuhn C, Moll R, Gould VE. Synaptophysin: a marker protein for neuroendocrine cells and neoplasms. Proc Natl Acad Sci U S A 1986;83:3500–4.
17. Abrahamsson PA. Neuroendocrine differentiation in prostatic carcinoma. Prostate 1999;39:135–48.
18. Sowalsky AG, Ye H, Bubley GJ, Balk SP. Clonal progression of prostate cancers from Gleason grade 3 to grade 4. Cancer Res 2013;73:1050–5.
19. Wilkinson S, Harmon SA, Terrigino NT, Karzai F, Pinto PA, Madan RA, et al. A case report of multiple primary prostate tumors with differential drug sensitivity. Nat Commun 2020;11:837.
20. Higano CS. Side effects of androgen deprivation therapy: monitoring and minimizing toxicity. Urology 2003;61:32–8.
21. Beltran H, Hruszkewycz A, Scher HI, Hildesheim J, Isaacs J, Yu EY, et al. The role of lineage plasticity in prostate cancer therapy resistance. Clin Cancer Res 2019;25:6916–24.
22. Norris JM, Carmona Echeverria LM, Bott SRJ, Brown LC, Burns-Cox N, Dudderidge T, et al. What type of prostate cancer is systematically overlooked by multiparametric magnetic resonance imaging? An analysis from the PROMIS Cohort. Eur Urol 2020;78:163–70.
23. Sowalsky AG, Ye H, Bhasin M, Van Allen EM, Loda M, Lis RT, et al. Neoadjuvant-intensive androgen deprivation therapy selects for prostate tumor foci with diverse subclonal oncogenic alterations. Cancer Res 2018;78:4716–30.
24. Davies AH, Beltran H, Zoubeidi A. Cellular plasticity and the neuroendocrine phenotype in prostate cancer. Nat Rev Urol 2018;15:271–86.
25. Cookson MS, Sogani PC, Russo P, Sheinfeld J, Herr H, Dalbagni G, et al. Pathological staging and biochemical recurrence after neoadjuvant androgen deprivation therapy in combination with radical prostatectomy in clinically localized prostate cancer: results of a phase II study. Br J Urol 1997;79:432–8.
26. McClintock TR, von Landenberg N, Cole AP, Lipsitz SR, Gild P, Sun M, et al. Neoadjuvant androgen deprivation therapy prior to radical prostatectomy: recent trends in utilization and association with postoperative surgical margin status. Ann Surg Oncol 2019;26:297–305.
27. Fair WR, Cookson MS, Stroumbakis N, Cohen D, Aprikian AG, Wang Y, et al. The indications, rationale, and results of neoadjuvant androgen deprivation in the treatment of prostatic cancer: Memorial Sloan-Kettering Cancer Center results. Urology 1997;49:46–55.
28. Karakiewicz PI, Eastham JA, Graefen M, Cagiannos I, Stricker PD, Klein E, et al. Prognostic impact of positive surgical margins in surgically treated prostate cancer: multi-institutional assessment of 5831 patients. Urology 2005;66:1245–50.
29. Caffo O, Maines F, Donner D, Veccia A, Chierichetti F, Galligioni E. Impact of enzalutamide administration on primary prostate cancer volume: a metabolic evaluation by choline positron emission tomography in castration-resistant prostate cancer patients. Clin Genitourin Cancer 2014;12:312–6.